Research Article

iMedPub Journals
www.imedpub.com

Advances in Applied Science Research
ISSN 0976-8610

2021
Vol.12 No.10:826

Modelling and Assessing the Spatiotemporal Changes to Future Land use and Climate Change Scenarios in the Mellegue Basin

Okba Weslati*

Department of Plant Science and Biotechnology, Faculty of Science, Ekiti State University, Ado-Ekiti, P.M.B 5363, Ekiti State, Nigeria

***Corresponding author:** Okba Weslati, Department of Biomedical Data Science, Geisel School of Medicine, Hanover, USA, Tel: 21886100; E-mail: okba.weslati@gmail.com

Received date: December 03, 2021; **Accepted date:** December 17, 2021; **Published date:** December 24, 2021

Citation: Weslati O (2021) Modelling and Assessing The Spatiotemporal Changes to Future Land Use and Climate Change Scenarios in the Mellegue Basin. Adv App sci res Vol:12 No:10.

Abstract

The watershed of Mellegue, which covers 10500 km^2, is a common area for Algeria and Tunisia. The catchment was chosen to predict future Land Use Land Cover (LULC) changes using GIS and remote sensing. Two future LULC scenarios have been generated using the Multi-Layer Perceptron (MLP) Markov Model of Idrisi. Afterwards we have tried to link the future response of climate changes to the predictable LULC scenarios. With the assistance of Python, we have produced four predictive weather change models. Forecasted models were based on the historical data generated from AquaCrop software. The predictive results have revealed a significant alteration of climate as a response for the great change that occurs in all of the LULC patterns.

Keywords: Watershed of Mellegue; LULC; MLP Markov; Idrisi; Climate change; Python

Introduction

LULC changes have been considered as an important item for global environmental changes. Understanding how the global environment and ecosystems responded to the past LULC changes may provide insight into the alteration that may cause these changes on the global environment. The earth surface is changing so rapidly, conversion of LULC grounds are linking to the persistent need for energy and food supplies which may exert a continuous pressure on terrestrial ecosystems as degrading water quality along with soil fertility, in addition to create many irretrievable phenomena such as desertification, water salinization, erosion as increasing the odds of destructive flood occurrences [1-3].

It was also seen that Climate alteration is sensible to LULC changes [4,5]. Due to the growth of human populations, LULC change impacts are mostly affecting the local weather climate. The weather of the study area, which belongs to the arid and semi-arid climate, is threatened by water scarcity. Indeed, the area is known to be shared by Algeria and Tunisia where they are both classified as extremely high stressed regions referring to more than 80 percent of the available water are been consumed annually [6]. Moreover, both countries have noticed a growth in human population in the last decade which compelled to a fast change in LULC fields to keep pace with the increasing demand for greater resources [6]. Certainly, this continuous growth of population, along with climate deterioration, May makes our region unable to compensate the required fundamental supplies. Therefore, it is essential for policy makers to understand and predict LULC changes in order to plan for a coordinated and controlled growth. The ability of humans to adapt to these rapid and unprecedented changes will also need to be tested during the coming decades. The manner in which we deal with population growth toward natural resources and regional economic development will certainly determine how we will respond toward future global change.

The response of human activities to environmental changes may be contingent on the productivity of the lands. On the other hand, rapid changes of LULC are related to the social, political and economic characteristics. For example, the agriculture of Tunisia is based on the production and exportation of oil olive. Algeria is rather based on the cultivation of olive and viticulture. Hence, the established strategies for these specific lands have caused a substantial rise in olive and viticulture during the last two decades. Consequently, these changes in land use may be detrimental in the degradation of land resources and the global environment at an unacceptable rate [7].

Besides their abilities in detecting and monitoring land use types at different scales, remote sensing and GIS have been proven as an effective alternative for predicting LULC and climate change scenarios [8-10]. One of the most efficient models used for long-term prediction is the MLP Markov chain model which simulates the spatial variation in a complex system. Its feasibility has been largely applied, at different scales, where the results were pretty much satisfied and promising [11,12].

It is found programming languages are being used for solving data science problems. Besides, the wide availability of current and past meteorological data has given the advantage of this software to manage the large amount of data with different types. Many environmental researchers are adapting the use of Python programming language in analyzing data science issues. Even though it seems often hard to predict the response of climate change to future Land uses conversion [13]. For that

reason, Python has provided several prediction algorithms that can be set depending on the types and the volume of the data, which can easily compare the quality of the applied machine learning model [14,15]. Accordingly, multiple future climate scenarios must be set at different scales to examine all potential likelihoods.

Based on these proofs, it is evident that human activities are threating the long-term stability of Earth's system as they are overriding natural changes to ecosystems brought by climate variations and land use changes.

Therefore, we must focus on the in luence on human impact by monitoring and predicting the LULC to assume future impacts of these changes on the environment, the ecosystem and the climate.

The present study was aimed irstly to forecast LULC changes in the Mellegue catchment using the MLP Markov Model; Secondly, to develop a set of climate change scenarios using Python programming so tware and inally to study the responses of these generated scenarios to the predicted LULC changes.

Study Area

Mellegue Catchment is located between 36° 25' 50.43", 35° 12'20.74" north and 7° 11'30.98", 8°55'7.99" east (Figure 1). It covers an area of 10500 km^2 while its perimeter is about 1053.8 km. Sixty percent of the catchment surface (6255.2 km^2) is located in Algeria where it starts in the Mounts of Tebessa, lows through the massif of Aures up to the southern end. But the outlet as well as the remaining area is situated in Tunisia where it follows the long mountains range of Tunisian Atlas which separates the north from the midland.

The so called Oued Mellegue is the main river of the catchment covering 282 km long.

It originates in the high plains along the northern hillsides of Nementcha massif near the village of Kenchela (Algeria) following the southwestern-northeastern direction of the Algerian-Tunisian Atlas until it ends in Jendouba (Tunisia) to join Oued Mejerda at the height of 140 m above sea level [16].

Morphologically, the basin holds a moderate to strong relief where the slope varies from 0 to 25%. The basin is known by the profusion of salt extrusions due to the faults' action that extrudes the Triassic evaporite and silicates. The study area is predominately covered with sedimentary rocks that illustrate a variety of different layers' age, mainly formed of limestone, marl, silts, alluvia and clay [17,18].

The basin contains a low variety of vegetation due to the semi-arid climate with a slight change to sub-arid in the north, characterized by hot-dry summer and cold winter that provides 50% of the annual rainfall.

Finally, the average temperature is estimated at 17°C annually with a slight variation of 1 to 2°C.

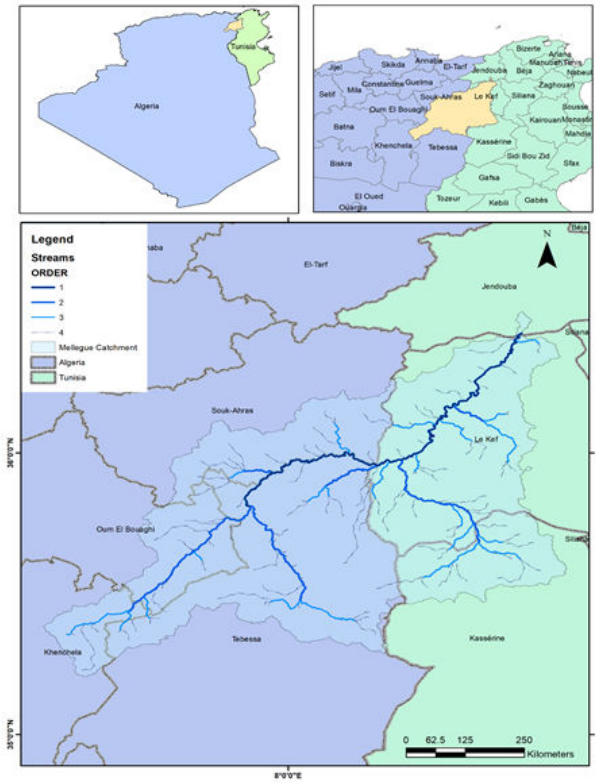

Figure 1: Location of the Study Area.

Materials and Data

LULC data

Past LULC change maps were attained based on Landsat 7 and 8 satellite images (Figure 2 and Table 1). The work was achieved using maximum likelihood classified from the supervised classification, classified into 9 classes: Unclassified, lake, vegetable crops, field crops, olive, viticulture, bare ground, forest and urban area. The two classified maps were based on the collected area of interests for each class.

The work required the assistance of GIS in treating, processing and managing both input and output data. Previously cited data and results where descripted meticulously, along with other complementary data (like change detection, NDVI and NDWI maps), in our previous article [17].

The two classification images are used as the basis for future projections. We succeeded in developing 2034 and 2050 LULC scenarios using Idrisi (TerrSet Selva 17.2). The model was based on neural network of the Markovian chain method of the Idrisi's Land Change Modeller (LCM). The neural network classifiers include a multi-layer perceptron and self-organizing maps that involves digital elevation model (DEM), distance from roads, distance from streams, distance from urban and slope map.

All maps were perfectly assessed and clipped according to the study area with ArcGIS software. As a final point, all cited data must be in the raster format with identical resolution and geographical extent.

Table 1: LULC spatial extent from 2002 and 2019.

Year	2002		2018	
Class	Area (km^2)	%	Area (km^2)	%
Lake	16.28	0.15	19.21	0.18
Arboriculture	952.21	9.03	619.07	5.87
Olive	850.28	8.06	1042.09	9.88
Vegetable crops	372.87	3.54	549.05	5.2
Field Crops	4507.37	42.76	5051.86	47.9
Forest	741.19	7.03	532.77	5.05
Urban Area	61.55	0.58	268.66	2.55
Bare Ground	3024.34	28.68	2042.17	19.39
Viticulture	10.75	0.1	411.95	3.91
Unclassified	7.16	0.07	7.16	0.07
Total	10544	100	10544	100

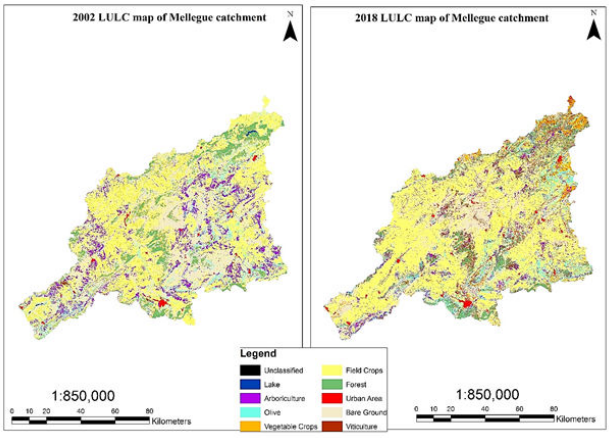

Figure 2: LULC change Map of 2002 and 2018.

Climate data

Daily weather data were collected all over the study area from 2002 to 2019. We succeeded in reassembling daily climate data from 22 stations distributed all around the catchment in order to conclude the fairest weather behaviour (figure 3). The data were used by AquaCrop software. It is open source software developed by FAO to understand the effect of environment and soils on crop production. At this stage, we would stop at the point of studying the effect of climate change based on the following historical weather data:

- Daily minimum (Tmin) and maximum (Tmax) temperature (°C).
- Daily rainfall (P) data (mm).
- Wind speed (m/s) data measured at 2 m above the soil surface.
- Daily relative humidity (fraction) known as vapour pressure deficit or saturation deficit.
- Solar energy (MJ/m²) or radiation data are either measured directly with radiometer or can be estimated based on the actual duration of sunshine using the Campbell-Stokes sunshine recorder.
- The station location (latitude and elevation) is also required to compute the day length and extra-terrestrial radiation.

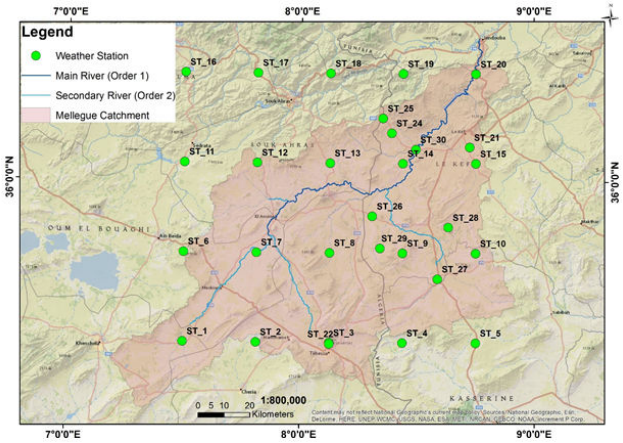

Figure 3: Weather stations in Mellegue catchment.

Results and Discussion

Aquacrop output

For each day of the simulation period, AquaCrop requires the historical weather climate data mentioned in the previous section. It computes:

Reference Evapotranspiration (ET0): The main purpose of ET0 is to assess the evaporative demand of the atmosphere based on weather data only. In AquaCrop, ET0 is computed according to the FAO Penman-Monteith equation given as follows:

$$Equation\ 1 \qquad ET_0\ (\mathrm{mm/day}) = \frac{0.408\Delta(Rn - G) + \Upsilon \frac{900}{T+273} U2\ (es - ea)}{\Delta + \Upsilon(1 + 0.34U2)}$$

Where

Rn: net radiation at the crop surface [MJ m-2 day-1], G: soil heat flux density [MJ m-2 day-1], T: air temperature at 2 m height [°C], U2: wind speed at 2 m height [m s-1], es: saturation vapor pressure [kPa], ea: actual vapor pressure [kPa], es–ea: saturation vapor pressure deficit [kPa], Δ: slope vapor pressure curve [kPa°C-1], Y: psychrometric constant [kPa°C-1].

Rainfall Data (P): rainfall data are presented either monthly or annually. Rainfall data are essential for AquaCrop to calculate soil water balance.

Average Tmin and Tmax: average Tmin and Tmax are presented in °C. In fact, these parameters can influence ET0 because air can easily transfer the heat energy to the crops.

Growing Degree Days (GDD): it is defined as the required mean temperature (Average Daily Minimum And Maximum Temperatures) and days for the crop to reach maturity. Computed GDD is based on the following equation

$$Equation\ 1 \qquad ET_0\ (\mathrm{mm/day}) = \frac{0.408\Delta(\mathrm{Rn} - \mathrm{G}) + \Upsilon \frac{900}{T+273} \mathrm{U2}\ (\mathrm{es} - ea)}{\Delta + \Upsilon(1 + 0.34\mathrm{U2})}$$

- Accumulated growing degree-day
- Maximum temperature
- Minimum temperature
- Is the base temperature and it is known as 5°C.

Based on the results of AquaCrop (Figure 4), we can see the fluctuation of weather parameters in the watershed of Mellegue; rainfall (P) oscillates between 400 and 600 mm/year with some exception in 2003, 2004 and 2009 where it has reached almost 700 mm. As for ET_0, it varies between 1250 and 1400 mm/year. It seems also that it behaves according to a specific periodic cycle; once it gets the maximum, it starts to decrease next until getting the next peak. As we can see here that ET_0 and P have the same periodic cycle but they are proportionally inversed. When P reaches the maximum, ET_0 is at the lowest level. As for Tmax, there has not been any considerable change during the study period where it goes around 22°C (±1°C). On the other hand, Tmin was on the average of 10°C from 2002 to 2010 and has declined to 8 °C from 2011 to 2019. As for GDD, it mainly depends from Tmin and Tmax where it goes around 3700 GDD. Based on the P results, it is evident that the study area is under a semi-arid climate [19]. Hence, the unbalanced annual precipitation has a serious effect on supplying water resources needed for agriculture which affects crop yields. On the other hand, semi-arid rainfalls have become shorter in time but extremely heavy that could generate floods [20]. Since 2012, ET_0 has noticed a significant decline which defines a specific aspect for semiarid area where they have noticed a decrease in annual evapotranspiration all around the world [21].

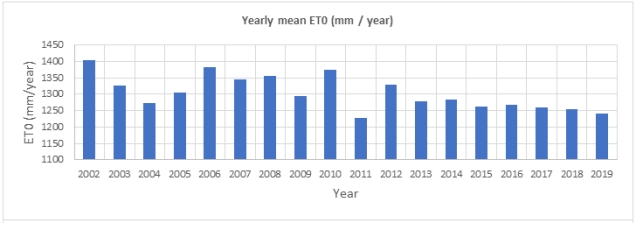

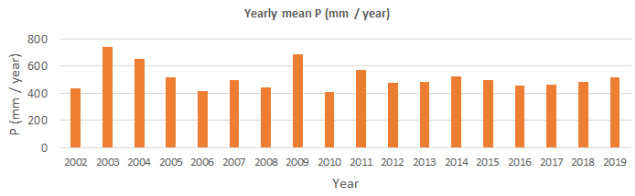

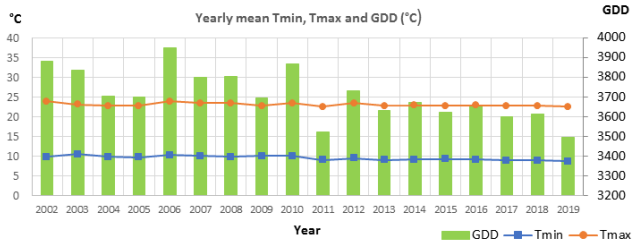

Figure 4: Yearly weather climate in mellegue watershed.

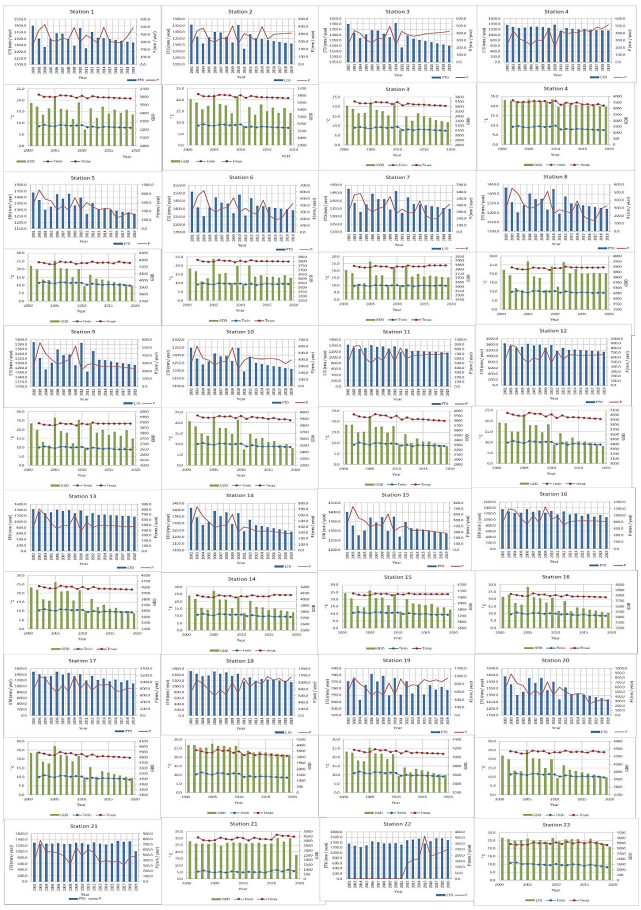

Figure 5: Yearly weather data of each station in mellegue catchment.

Predicting LULC change

First Scenario

Predicting LULC change model was operated using the LCM of Idrisi TerrSet. The process requires 2002 and 2018 LULC maps. The generated change map between 2002 and 2019 was very complex, so we had to study only major changes because the model does not accept more than nine transition events. Therefore, we had to ignore transition zones that are less than 2% (200 km^2) of the total area [22,23]. Enhanced change map has given eight majors transitions events illustrated in the following figure.

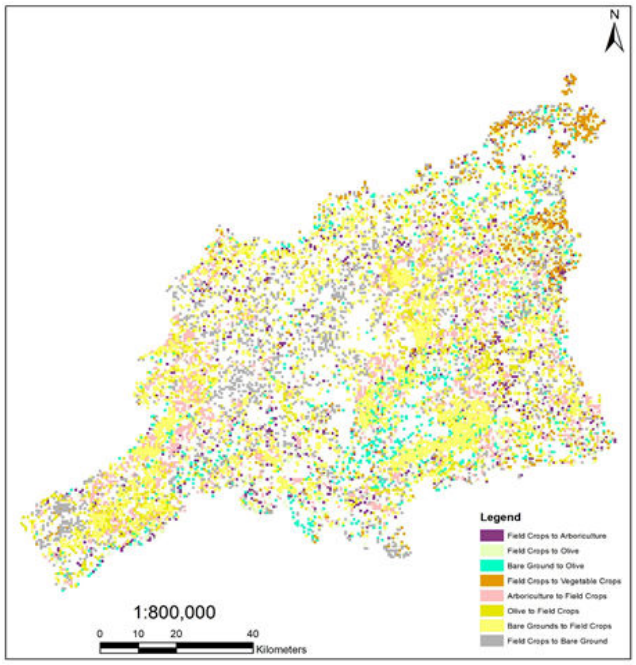

Figure 6: Enhanced Change Map detection from 2002 to 2018.

MLP neural network were applied afterward to build an algorithm based on the training data of the resultant transition map. The accuracy rate and RMS errors were given based on the selected training samples that were randomly selected for each transition zone. Results has given an accuracy rate of 75% and RMS of 0.16 where the validity was supported by proving that acceptable accuracies are those closed to 80%. Later on, the Markov chain was applied to generate future LULC maps [24]. Transition probabilities for each land cover category are converted into a resulting matrix. This transition matrix will be followed by the projection of future LULC where statistics and maps are given in Table 2 and Figure 7.

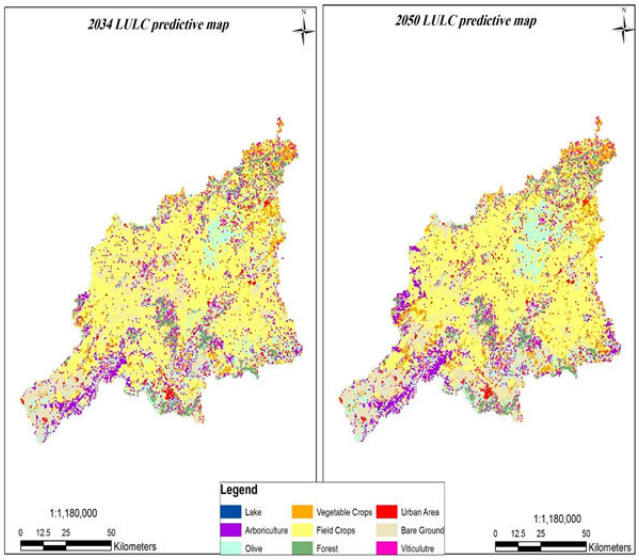

Figure 7: 2034 and 2050 predictive LULC maps.

Table 2: 2034 and 2050 predictive LULC areas.

Class	2034 area	2050 area
Unclassified	169.33	169.33
Lake	18.42	18.42
Arboriculture	590.28	568.63
Olive	1112.71	1196.72
Vegetable Crops	667.18	795.76
Field Crops	4892.84	4822.08
Forest	520.49	520.49
Urban Area	268.49	268.49
Bare Ground	1901.69	1781.51
Viticulture	402.57	402.57
Total	10544	10544

The first scenario shows a general stability of some classes; there is small increase in lake from 16 km^2 in 2002 to 18.42 for 2034 and 2050. It has been a small change for field crops as it slightly decreases from 5051 km^2 in 2018 to 4892 km^2 in 2034, to finally achieve 4822 km^2 in 2050. It is quite the same for viticulture as it declines from 411 km^2 in 2018 to 402 km^2 for both 2034 and 2050. Forest has witnessed also a shrinking in area, from 532 km^2 in 2018 to 520 km^2 for both 2034 and 2050 periods. As for urban area, there have not been any changes as it remains 268 km^2 from 2002 to 2050. The rest of classes have noticed a remarkable change in area as we observe a growth in olive from 1042 km^2 in 2002 to 1112 km^2 in 2034 as it reaches 1196 km^2 in 2050. Vegetable crops have also been increasing where it gets 667 km^2 in 2034 and 795 km^2 for 2050 compared to 549 km^2 in 2018. The general decline of arboriculture, from 952 km^2 in 2002 to 619 km^2 in 2018, is so far proceeding as it goes from 590 km^2 in 2034 to 568 km^2 in 2050. The most important change has occurred for bare ground as it changed from 2042 km^2 in 2002 to 1901 km^2 in 2034 as it finally achieves 1781 km^2 in 2050. It is quite understandable considering the non-changes in lakes, viticulture and especially urban area because the built predictive model was based on the historical transition change map that happened from 2002 to 2018. This is one of the major limited issues of MLP- Markov in LCM, where no more than nine transition maps can be tolerated or processed. The big density and the evolution of the classes in such a large area has oblige us to ignore some of the most important transition events especially the urban area since we do all know the impact of conversion in urbanized areas for the environment and the climate. This point will limit policy makers and environmentalist to make the suitable intervention for preserving the watershed resources.

In the meanwhile, based on the results of the first model with the exception of arboriculture, we do realize, generally, a rise in agricultural lands (field crops, vegetable crops, olive and viticulture) as they recorded 7075 km^2 in 2034 and 7216.96 km^2 for 2050 where they were only 5741 km^2 and 7054 km^2 in 2002

and 2018, respectively. Because the total area is always unchangeable and there were not any other considerable changes, we can conclude that the most important transition has occurred from bare ground to agricultural lands. It is found that agricultural have been considered as major threat for the environment, ecosystem and humans. Agricultural yields are strongly linked to the application of pesticide and nutrient. These substances are responsible for eutrophication in surface water, which is caused due to the nutrient enrichment in water. One of the most relics of eutrophication is the abundance of algal bloom, causing degradation in the drinking water taste and odor. Besides their undesirable reproduction, these algal are threating aquatic species because they are very toxic once they have been digested. On the other hand, the abondance of the pesticide and manure are degrading the ground water quality. Once these fertilizers are been infiltrated by the soil, they will excessively poison the ground water in nitrogen and phosphorous. Yet, human life is also been threating where many syndromes have been the origin of toxic drinking water rich in pesticide substances and phosphorous [25-27]. The agricultural land can also affect to quality of the soil by modifying their original components [28]. Hence, associated agricultural activities can significantly affects areas that are situated far away from their place of origin [29]. At last, rising and abundance of agricultural lands does not provide food security because they are not equally distributed [30].

Second scenario

As seen in the previous section, the first model has taken in consideration only the most important transition events to build the predictive maps and statistics. On the other hand, the second scenario has applied a forecasting model for each class apart. Based on the obtained results we can distinguish that the first scenario does not take in consideration the historical evolution of some classes. For example, if we have an insight look of the evolution of field crops from 2002 to 2018, we do observe that the percentage of occupying area has been expanding from 42% (4507km^2) to 48% (5052km^2), correspondingly. Based on this behavior, we could assume that this land use category will continue in increasing for future year. In the opposite, any considerable changes for field crop have not occurred (almost stable), neither for 2034 or 2050. This fact was considered as second incapacities for the first scenario where the model has been exclusively relying on transition map to predict future outcomes. The second scenario was rather based of the general trend for each class separately. So, in the following section, we could conclude that all the data have been convenient compared to the historical behavior for every class.

Lake

Based on the following results (Table 3), lakes area has been decreasing from 19 km^2 in 2018 to 10 km^2 in 2034 and only 1 km^2 in 2050. The following map (Figure 8) is showing the distribution of water surface all around the catchment. As we see, lake spots are being poorly distributed especially for 2050. It is also known that our study area belongs to regions under high water stress. So, based on the following consumption of water resources, it is obvious that the area will suffer from water scarcity in so many levels (agriculture, drinking water, industries). Besides human, fauna and flora that are the most dependent on water, one of the most important vulnerable sectors for water drought is agriculture. In fact, under water stress conditions, plants have developed several physiological responses and complex mechanisms that have significantly influenced the crops at their development stages and that can lead to an important decrease in the crops yield, including the decline of their quality [31-33].

Table 3: Area statistics of forecasted lakes in 2034 and 2050.

Class	2034 area	2050 area
Unclassified	169.33	169.33
Lake	10.02	1.62
Arboriculture	612.25	612.57
Olive	1029.68	1030.65
Vegetable Crops	538.91	539.23
Field Crops	4967.8	4972
Forest	520.49	520.49
Urban Area	268.81	269.13
Bare Ground	2023.82	2025.76
Viticulture	402.9	403.21
Total	10544	10544

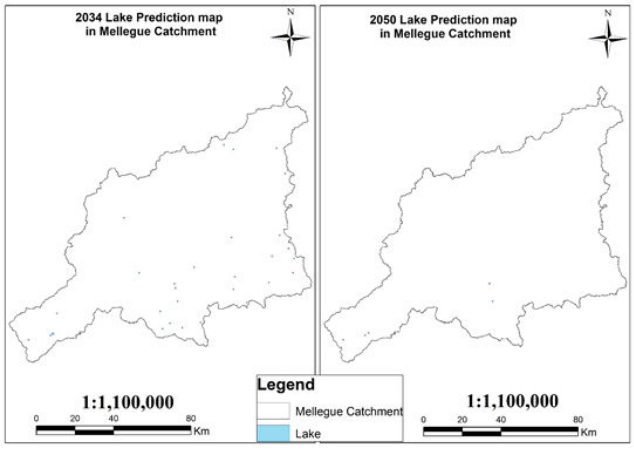

Figure 8: Predictive lake map in 2034 and 2050.

Arboriculture

Arboriculture lands are still decreasing over time as they reached 323 km^2 in 2034 compared to 619.07 km^2 in 2018 (Figure 9, Table 4). They nearly vanished in 2050 getting almost 35 km^2 of area. Based on the current governmental strategies, it is quite reasonable for arboriculture to decline; Tunisia is

developing an encouraging strategy for olive plantation. As for Algeria, it based on the plantation of olive and viticulture [34,35]. Hence, arboriculture areas are linked directly to the water resources as one hectare of arboriculture need approximately 3000 cubic meters of irrigated water [36]. That amount cannot be affordable for water stressed regions such as Tunisia and Algeria. The situation is been aggravating due to the arid and semi-arid climate that does not support arboriculture and orchards.

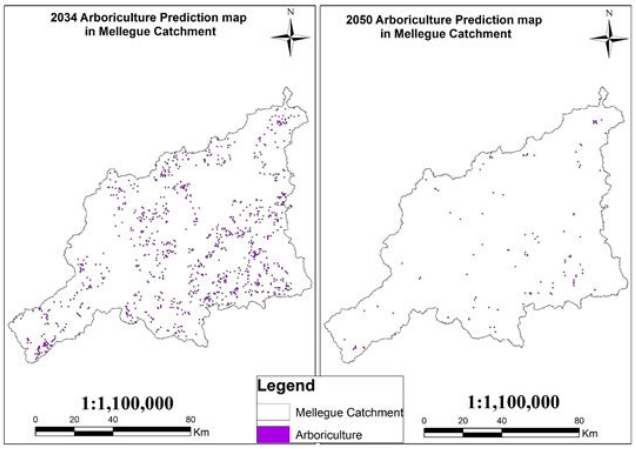

Figure 9: Predictive arboriculture map in 2034 and 2050.

Table 4: Area statistics of forecasted arboriculture in 2034 and 2050.

Class	2034 area	2050 area
Unclassified	169.33	169.33
Lake	18.74	19.06
Arboriculture	323.41	34.89
Olive	1058.76	1088.81
Vegetable Crops	554.42	570.25
Field Crops	5123.52	5283.45
Forest	528.248	536
Urban Area	278.82	289.16
Bare Ground	2076.81	2131.73
Viticulture	411.94	421.31
Total	10544	10544

Olive and Viticulture

Olive have continued in increasing as they reach 1481 km^2 in 2034 and 1933 km^2 in 2050 compared to 1042 km^2 in 2018 (Figure 10 and Table 5). As for viticulture, they used to be 411 km^2 in 2018 as they extend to 578 km^2 in 2034 and finally achieve 754 km^2 in 2050 (Figure 11 and Table 5). We do know that Tunisia rely mostly on olive cultivation. In fact, 30% of Tunisian lands are dedicated to olive plantation [37]. Furthermore, European Union has declared that they reached a record in imported Tunisian oil olive [38]. Development strategies are still firm by the government to encourage farmers for olive cultivation or oil olive industries. Besides their 34 000 000 ha dedicated for olive plantation, Algeria is ranked as second wine producer and fifth wine exporter in Africa [39]. With more than 1,000,000 ha for grapes growth. So, if we compare them to the 48 000 km^2 of Tunisian viticulture lands, we can presume the importance of viticulture growing and industry for Algeria [40].

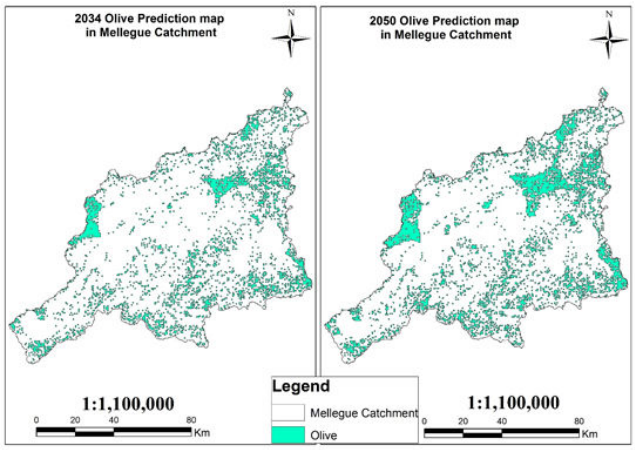

Figure 10: Predictive Olive map in 2034 and 2050.

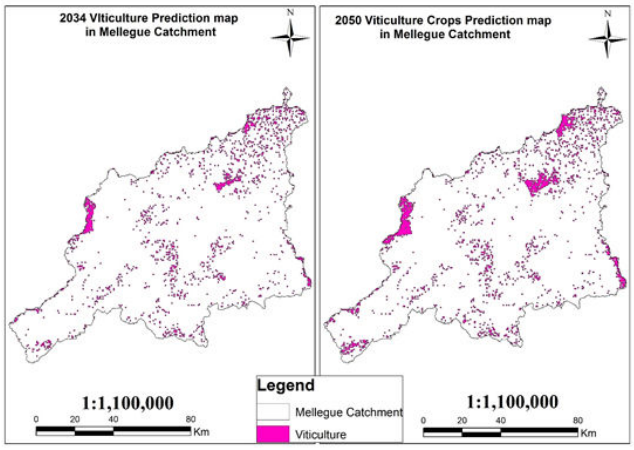

Figure 11: Predictive viticulture map in 2034 and 2050.

Table 5: Area statistics of both forecasted olive and viticulture in 2034 and 2050.

	Forecasted Olive scenario		Forecasted Viticulture scenario	
Class	**2034 area**	**2050 area**	**2034 area**	**2050 area**
Unclassified	169.33	169.33	169.33	169.33
Lake	17.45	16.48	18.09	17.77

Arboriculture	581.88	551.83	602.56	593.19
Olive	1481.03	1933.36	1011.26	993.82
Vegetable Crops	512.427	486.25	527.6	516.62
Field Crops	4723.54	4483.49	4883.15	4802.7
Forest	495.62	470.74	504.34	488.19
Urban Area	254.92	241.35	263.96	259.44
Bare Ground	1924.31	1826.74	1985.37	1948.86
Viticulture	383.51	364.44	578.33	754.09
Total	10544	10544	10544	10544

Vegetable Crops and Field Crops

Vegetable crops have been rising according to following results (Figure 12, Table 6), where they get 775 km^2 in 2034 as they used to be 550 km^2 in 2018. They keep expanding to achieve in 2050 an area of 1011 km^2. As for field crops (Figure 13, Table 6), they jumped from 5052 km^2 in 2018 to 6234 km^2 in 2034 and 7506 km^2 in 2050. Vegetables and field crops have been always linked the human growth. Consistent demand for food has always led to the cultivation of cereals and vegetables for daily consumption. To get along with the urban extension, associated with demographic growth, vegetable and field crops must always be cultivated to achieve the certain equilibrium between human rise and food.

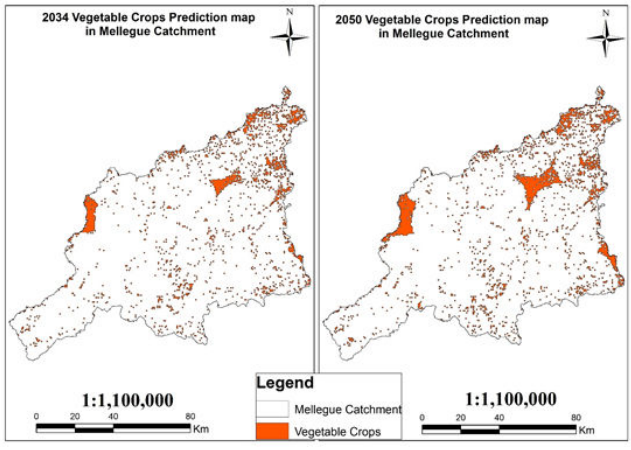

Figure 12: Predictive vegetable crops' map in 2034 and 2050.

Table 6: Area statistics of both forecasted vegetable and field crops in 2034 and 2050.

	Forecasted vegetable crops' scenario		Forecasted field crops scenario	
Class	**2034 area**	**2050 area**	**2034 area**	**2050 area**
Unclassified	169.33	169.33	169.33	169.33
Lake	18.09291	17.76982	14.21586	10.01572
Arboriculture	596.0968	580.2655	451.9997	292.0713
Olive	1003.833	978.9557	775.0873	521.4635
Vegetable Crops	774.7643	1010.941	414.8446	291.102
Field Crops	4835.007	4706.418	6234.623	7505.65
Forest	508.54	496.5858	426.1526	331.811
Urban Area	263.9626	259.4394	220.6689	172.8519
Bare Ground	1971.804	1921.726	1538.22	1054.558
Viticulture	402.5672	402.5672	298.8561	195.145
Total	10544	10544	10544	10544

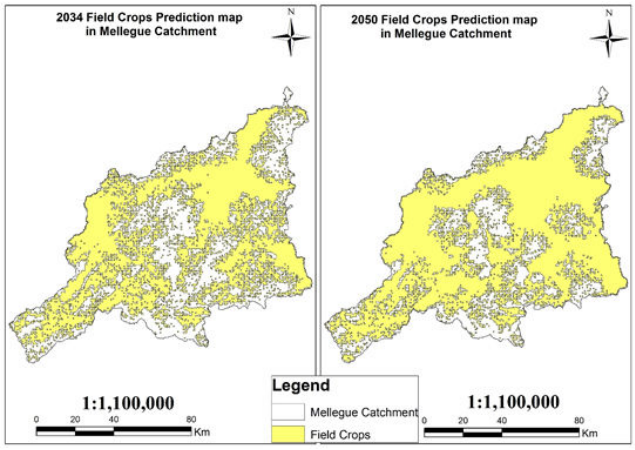

Figure 13: Predictive field crops' map in 2034 and 2050.

Forest

According to following results (Figure 14 and Table 7), Forest occupied and area of 533 km^2 in 2002 have decreasing gradually to 296 km^2 in 2034 and only 72 km^2 in 2050. Beside the rigid climate that is playing a key factor for forest survivals, one of the main reasons to forest degradation is urban expansion. The advance of technology associated with demographic growth has developed the trades in forestry products, which degrade considerably forest areas [34,41]. In fact, more than 4,00,000 cubic meters of wood have been produced from Tunisian forests. Yet, forests lands where severely reduced since the 2011 socio-political revolution [42]. As for Algeria, deforestation has severely daSmaged forests where they recorded a deforestation rate of 18000 ha/year in 2018 compared to 11000 ha/year in 2005 [43].

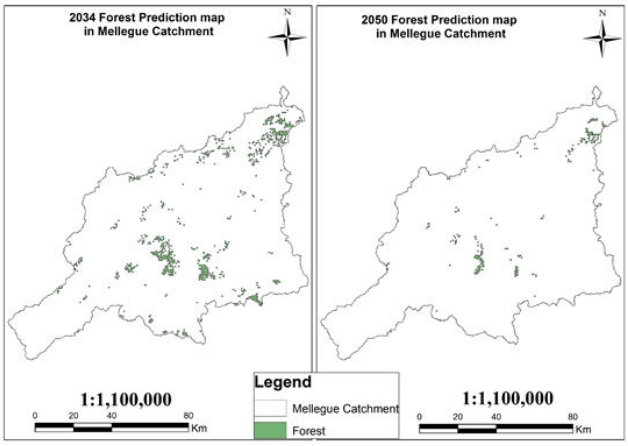

Figure 14: Predictive forests' map in 2034 and 2050.

Table 7: Area statistics of both forecasted Forests in 2034 and 2050.

Class	2034 area	2050 area
Unclassified	169.33	169.33
Lake	18.73909	19.06217
Arboriculture	628.4055	644.883
Olive	1053.589	1078.467
Vegetable Crops	550.5414	562.4956
Field Crops	5057.938	5152.279
Forest	296.2714	72.04855
Urban Area	275.5938	282.7017
Bare Ground	2074.869	2127.855
Viticulture	418.7216	434.876
Total	10544	10544

Urban Area and bare grounds

Urbanized areas have showed a considerable increase compared to the recorded 268 km^2 in 2018 (Table 6), where they reach 428 km^2 in 2034 as they finally achieve 588 km^2 in 250. The following map (Figure 15) illustrated the evident spread of urban areas all over the years. Urban expansion is directly associated with demographic growth. Indeed, predictive assumption for world population has claimed a value of 9.3 billion in 2050 compared to 7.5 billion in 2020 [34]. This will lead to an increase in food demand, which will indirectly support agricultural lands expansion (except for arboriculture). Moreover, population growth will ultimately affect forests as the consumption of forestry products are being industrialized. The following map (Figure 17) was built by overlaying all forecasted maps for each class. We could remark the most probable converted lands into agriculture, which they seem to refer as bare ground. Based on this factor, we conclude that bare grounds are the most vulnerable lands that could be easily converted. Besides, expansion of urbanized areas and agricultural lands will automatically decrease bare grounds' area. In fact, our model (Figure 16, Table 8) states that bare grounds will be 1215 km^2 in 2034 and only 409 km^2 in 2050, when they were 2042 km^2 in 2002.

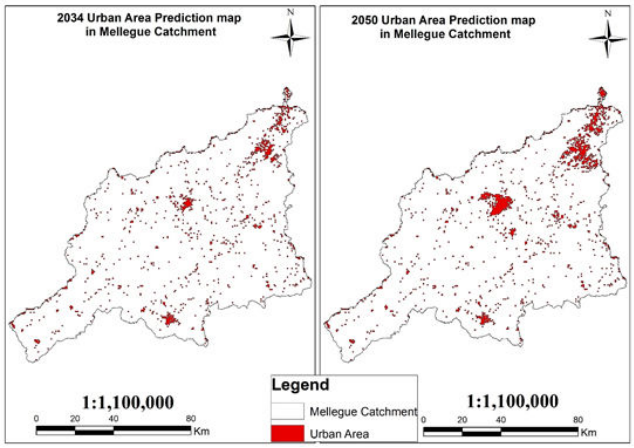

Figure 15: Predictive urban areas' map in 2034 and 2050.

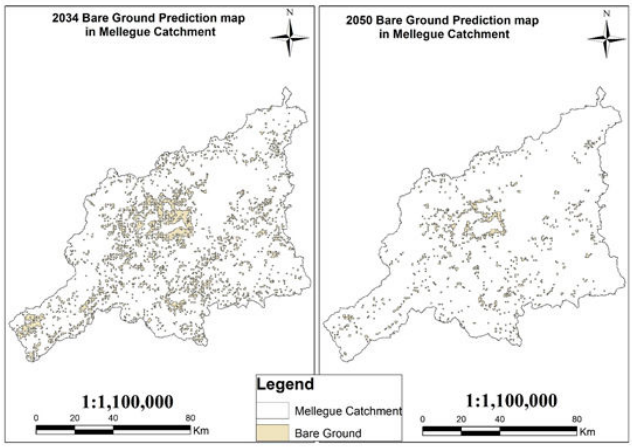

Figure 16: Predictive bare grounds' map in 2034 and 2050.

Table 8: Area statistics of both forecasted urban areas in 2034 and 2050.

	Forecasted urban area scenario		Forecasted bare grounds' scenario	
Class	**2034 area**	**2050 area**	**2034 area**	**2050 area**
Unclassified	169.33	169.33	169.33	169.33
Lake	18.09291	17.76982	20.03144	21.64687
Arboriculture	601.5893	591.2504	669.4377	726.9473
Olive	1009.972	991.233	1126.284	1223.856

Vegetable Crops	529.8638	521.1404	588.6657	638.7443
Field Crops	4892.517	4821.437	5447.258	5930.92
Forest	513.3863	506.2784	563.1418	605.7894
Urban Area	428.4143	588.3427	305.3179	342.1499
Bare Ground	1985.051	1948.219	1215.456	409.029
Viticulture	395.7824	388.9976	439.0762	475.5851
Total	10544	10544	10544	10544

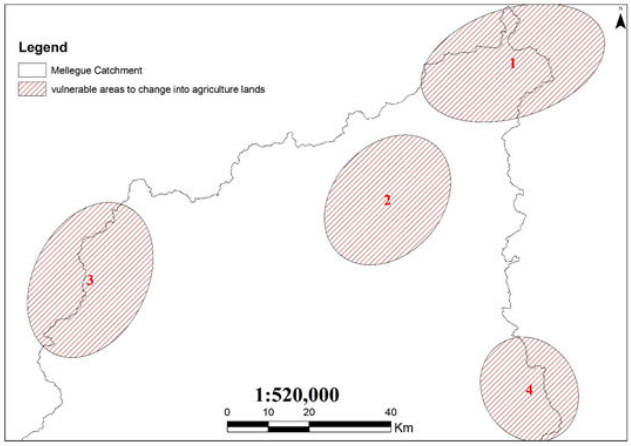

Figure 17: Most likely converted lands into agriculture.

Forecasting weather climate using Python

Linear Regression is considered as one of the most famous fundamental tools in predictive analytics [15]. Linear Regression has been applied for our case study where we have developed several models where year column corresponds to independent variable.

Scenarios I: Simple (or multiple) Linear Regression (LRM)

In this model we have developed a single linear equation with two dimensional variables; the independent variable (x) concerning the year and the dependant variable (Y) referring to weather parameter (ET_0, P, Tmin, Tmax or GDD). The model runs according to the following equation:

Equation 3

$$Y = \alpha + \beta x$$

Where Y: weather parameter, x: year, α: intercept, β: slope

The simple difference between multiple and simple linear regression is founded in the use of more than one independent variable. In this case. the equation will be:

Equation 4

$$F\ (x_1 \ldots . x_r) = b_0 + b_1 x_1 + \cdots + b_r x_r$$

In the present study. we have only one independent variable which is the year. So, in that case multiple linear regressions will have the same results as the simple linear regression model. The future behaviour of the weather climate is revealed on the following section.

Scenarios II: Polynomial Linear Regression (PRM)

The polynomial regression runs according to the independent variable x (year) and the dependant variable Y (weather parameter) according to n polynomial degree. Therefore. The regression function has the following equation:

Equation 5

$$Y = \alpha + \beta_1 x + \beta_2 x2 + \ldots + \beta_n\ xn$$

Hence, second polynomial degree was found to the most appropriate (n=2). Predicted future responses are illustrated in the following section.

Scenario III and IV: Linear (PLRM) and polynomial (PPRM) regression based on the Pearson correlation

In order to get the general behavior of the catchment. we have chosen to repeat previous scenarios but with the assistance of Pearson correlation. We have to test the correlation of the data based on the Pearson coefficient. This correlation is based on the linear relation between the dependent variables. The coefficient range between -1 and 1 where values close to 1 represent a strong correlation. In this case. all stations with less than 0.6 have been neglected [44].

ET0

Predictive models have showing a general decrease in ET_0 as compared to 1250 mm/year in 2019 (Figure 8). The coefficients of both operated models (linear and polynomial regression model) are shown in the following Table 9. LRM has the more realist prevision as it indicates a value of 1150 mm/year in 2034 and 1044 mm/year in 2050. As for PRM, it shows a serious decline as it indicates that in 2034, ET_0 will be 1060 mm/year and only 800 mm/year in 2050. PLRM have indicated a forecasted ET_0 value of 1100 mm/year in 2034 and 980 mm/year in 2050, while PPRM has indicated that ET_0 will reach 990 mm/year in 2034 to finally achieve 635 mm/year in 2050. One of the most influenced factors for reference evapotranspiration is temperature and wind. Second scenario of land use prediction has confirmed a serious increase in urban area which will lead the increase of mean temperature. In fact, future assumption about the increase of temperature will be in the average of 1 to 5°C. Therefore, as the temperature rises, ET_0 will inversely decrease and that what is known as "Evaporation paradox" [45,46]. Hence, as the second LULC scenario claims, the rise in urbanized area will undoubtedly generated more polluted air. Well, it seems that air pollution have a negative impact responsible for the decreasing of ET_0 [47]. Additionally, second

LULC scenario proclaims a serious drought in water resources that could serve for irrigation. So, with the elevation of future mean temperature and the small contribution of semiarid climate in annual rainfall, crop yield will be considerably touched that could indirectly decreases annual ET_0 [48].

Table 9: Coefficients of ET_0 predictive models.

station	Linear			Poly (degree = 2)				Pear Corr
	R^2	Alpha (intercept)	Beta (slope)	R^2	alpha	Beta 1	Beta 2	
1	0.424	6647.688	-2.609	0.442	71982.19	-67.603	0.016	valid
2		10331.51	-4.465		-135589	140.694	-0.036	valid
3		18445.97	-8.537		-898740	903.865	-0.227	valid
4		21207.94	-9.93		-1260271	1264.865	-0.317	valid
5		16629.34	-7.606		-1060165	1063.572	-0.266	valid
6		6097.11	-2.327		-182580	185.367	-0.047	valid
7		8288.199	-3.434		-355145	358.103	-0.09	valid
8		7345.188	-2.981		-333614	336.2	-0.084	valid
9		6171.48	-2.414		-306579	308.705	-0.077	valid
10		11842.75	-5.263		-856433	858.485	-0.215	valid
11		29572.67	-14.073		-1394177	1402.25	-0.352	valid
12		31130.03	-14.848		-1436811	1445.436	-0.363	valid
13		27313.77	-12.944		-1245119	1252.851	-0.315	valid
14		16907.81	-7.759		-878430	882.91	-0.222	valid
15		8155.303	-3.399		-520074	522.075	-0.131	valid
16		25310.32	-11.982		-2341253	2342.237	-0.585	valid
17		40718.9	-19.604		-2708961	2715.734	-0.68	valid
18		41349.32	-19.909		-856518	873.275	-0.222	valid
19		2227.537	-0.629		-36331.8	37.729	-0.01	valid
20		16629.34	-7.606		-1060165	1063.572	-0.266	valid
21		-6340.02	3.794		2746547	-2734.73	0.681	invalid
22		-27551.3	14.4		316197.8	-327.556	0.085	invalid

$$Y = \alpha + \beta_1 x + \beta_2 x2 + ... + \beta_n xn$$

Figure 18: Predictive ET_0 scenarios.

P

Based on the following results (Table 10 and Figure 19), two plausible scenarios are identified here; Starting from 505 mm/year in 2019, LRM have declared a general decrease in P values where it will be 390 mm/year in 2034 and will finally attempt 315 mm/year in 2050. With PLRM, P values will get 267 mm/year in 2034 and 309 mm/year by 2050. PPRM has the most convenient trend because rainfalls have generally a very sensitive behavior in semiarid climate. With the announced results, we could say that we are still under a semiarid climate.

On the other hand, PRM has declared a signi icant elevation in P values where they will attain 637 mm/year in 2034 as they will exceed 1000 mm/year in 2050. Inversely, the application of PPRM has shown a decreased in P where they will be 346 mm/year in 2034 and 395 mm/year in 2050.

It is not easy to forecast rainfall because of its too sensitive behavior due to many climate variables (Temperature, Evapotranspiration, etc.,) and others (LULC change). Assessment of the polynomial rise in rainfall could be explained by the nature of semiarid weather, where rainfalls are too much inconstant. Yet, semiarid climate is known with high seasonal concentration of precipitation. Infiltration of water surface will be minimized due to urbanized ground. Consequently, with the reduction of vegetative covers (forests) runoff will be very high causing an important amount of erosion.

Such impact has a major effect on the soil environment as well as on the landscapes [49]. For the three other models (LRM, PLRM and PPRM), it is very likely that the region will be warmer due to the expansion of urbanized areas and the degradation of forests (second scenario of LULC). As a result, temperature will increase and more evaporation will occur which will automatically cause a high intensity and long periods of drought. On the other hand, sensible arid and semiarid areas will be much warmer than others temperate and wet regions.

Hence, future predictions claim that the Mediterranean regions will have a considerable loss of precipitation by the year 2100 [49].

Table 10: Coefficients of P predictive models.

station	Linear			Poly (degree = 2)				Pear Corr
	R^2	Alpha (intercept)	Beta (slope)	R^2	alpha	Beta 1	Beta 2	
1	0.24	1314.733	-0.471	0.45	1955249	-1944.21	0.483	invalid
2		-5584.91	2.966		613267.9	-612.659	0.153	invalid
3		-10413.2	5.361		715018.7	-716.287	0.179	invalid
4		-24202.1	12.224		2811409	-2808.6	0.702	invalid
5		45247.55	-22.258		-362350	383.213	-0.101	valid
6		19454.05	-9.497		2694180	-2670.27	0.662	valid
7		19175.88	-9.361		2680736	-2657.04	0.658	valid
8		24455.52	-12.007		2108146	-2084.83	0.515	valid
9		22382.37	-10.977		572407.1	-558.133	0.136	valid
10		4061.542	-1.82		315977.7	-312.109	0.077	valid
11		-2305.73	1.48		2445105	-2433.17	0.605	invalid
12		1374.014	-0.366		3188165	-3170.53	0.788	valid
13		17387.34	-8.389		2497309	-2475.38	0.614	valid
14		35750.21	-17.579		1209764	-1185.47	0.29	valid
15		34266.02	-16.841		1464560	-1439.67	0.354	valid
16		24775.85	-11.878		-60451	72.904	-0.021	valid
17		18649.56	-8.839		-1642844	1643.988	-0.411	valid
18		-41047.7	20.878		6646561	-6631.85	1.654	invalid
19		-26721.2	13.67		8793045	-8760.09	2.182	invalid
20		47094.68	-23.178		-1108226	1126.116	-0.286	valid
21		21667.25	-10.537		449278	-33.671	0.006	valid
22		-9415.84	4.774		4539127	-4520.04	1.125	invalid

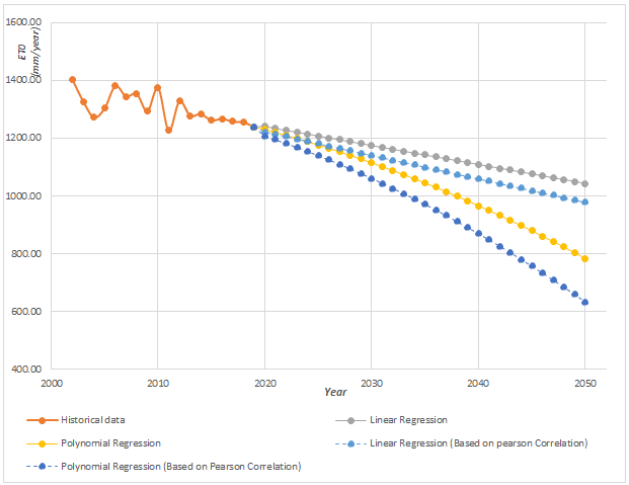

Figure 19: Predictive rainfall (P) scenarios.

Tmax and Tmin

According to the Tmax results in table 11 and figure 20, LRM has a future stabilized tendency. Future Tmax values have indicated 21.9°C in 2034 and 21.2°C in 2050. The results are pretty much close to the 22.5°C recorded in 2019. PRM have indicated a similar behavior to the LRM with slight decrease as it indicates 21.2°C in 2034 and 19.5°C in 2050. Regarding Pearson correlation, both applied models have confirmed a rise in annual temperature where the PLRM have indicated a future Tmax value of 25.4°C in 2034 and 26.2°C in 2050. PPRM have high Tmax values estimated of 27°C in 2034 and 31°C in 2050.

Concerning future Tmin (Figure 21 and Table 12), it will be decreasing in analogy to 2019 (8, 6°C). LRM has stated a future Tmin of 7.42°C in 2034, compared to 6°C in 2050. PLRM has stated 7.2 °C in 2034 and 5.6 °C in 2050. As for PRM, it mentions that Tmin will get 5.9°C in 2034 where it significantly declines in 2050 getting only 1.7°C in. Furthermore, PPRM model has estimated a 2034 Tmin of 5.19°C and no more than -0.42°C in 2050.

If we considered that average temperature is Tmean= (Tmin +Tmax)/2, we will conclude that temperature will increase during the study period. That seems to match previous assumption that claims future temperature will rise from 1 to 5°c [46]. In the other hand, any conversion in land to urbanized areas will automatically lead to the rise in surface temperature. The phenomenon will be intensified with water resources shortage related to the arid or semiarid climate, in addition to low vegetation cover [50]. This hypothesis fit perfectly with the second LULC scenario where it indicates a significant increase of urban areas, a diminution in forest areas as well as water surface resources (lakes). In addition, expansion in urban areas will trend to intensify the phenomenon of "urban heat island" and rise, subsequently, the Tmean as well as fluctuating Tmin and Tmax values [51,52]. In fact, Tmean values are expected to be higher in 2 to 5°C compared to the surrounding rural areas [53].

Table 11: Coefficients of Tmax predictive models.

station	Linear			Poly (degree = 2)	Pear Corr			
	R^2	Alpha (intercept)	Beta (slope)	R^2		alpha	Beta 1	Beta 2
1	0.437	155.859	-0.067	0.467	-4980.173	5.042	-0.001	invalid
2		180.185	-0.079		-9726.882	9.776	-0.002	invalid
3		244.728	-0.111		-14511.587	14.568	-0.004	invalid
4		280.637	-0.129		-23027.041	23.057	-0.006	invalid
5		-2.950	0.013		-2610.073	2.607	-0.001	valid
6		53.924	-0.016		-1249.637	1.281	0.000	invalid
7		-99.538	0.061		31420.577	-31.295	0.008	valid
8		-75.899	0.049		5659.772	-5.656	0.001	valid
9		-43.565	0.033		4127.832	-4.116	0.001	valid
10		190.673	-0.084		-29400.171	29.353	-0.007	invalid
11		340.335	-0.158		-20620.933	20.694	-0.005	invalid
12		316.858	-0.147		-18063.359	18.138	-0.005	invalid
13		204.082	-0.090		-12779.390	12.826	-0.003	invalid
14		-84.168	0.054		35242.347	-35.089	0.009	valid
15		-4.056	0.014		-499.410	0.506	0.000	valid
16		238.698	-0.108		-15299.754	15.350	-0.004	invalid
17		332.626	-0.154		-21567.206	21.631	-0.005	invalid
18		394.691	-0.185		-17724.813	17.840	-0.004	invalid
19		259.261	-0.118		-17130.249	17.181	-0.004	invalid
20		-2.950	0.013		-2610.073	2.607	-0.001	valid
21		-247.992	0.138		63652.590	-63.429	0.016	valid
22		-124.405	0.073		-20955.317	20.796	-0.005	valid

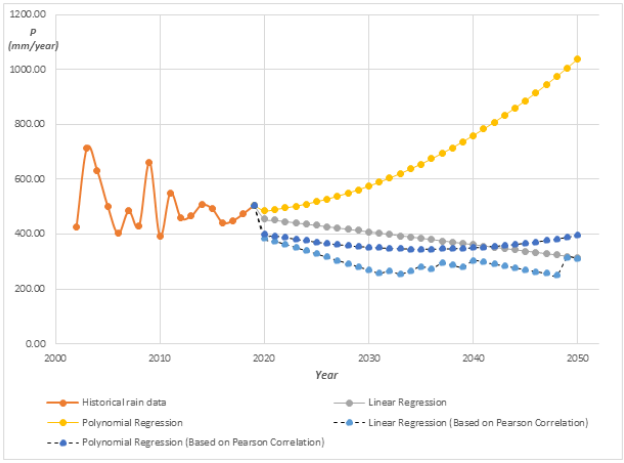

Figure 20: Predictive Tmax scenarios.

Table 12: Predictive Tmin scenarios.

station	Linear			Poly (degree = 2)	Pear Corr			
	R^2	Alpha (intercept)	Beta (slope)	R^2	alpha	Beta 1	Beta 2	
1	0.607	137.991	-0.064	0.648	-15061.5	15.056	-0.0038	valid
2		173.611	-0.082		-15104.1	15.116	-0.0038	valid
3		224.046	-0.107		-16539.8	16.569	-0.0041	valid
4		260.752	-0.125		-19188.4	19.222	-0.0048	valid
5		243.493	-0.116		-17771.7	17.806	-0.0045	valid
6		26.906	-0.009		-1198.44	1.21	-0.0003	invalid
7		24.705	-0.007		1745.406	-1.719	0.0004	invalid

8		110.243	-0.05		-15167.5	15.148	-0.0038	valid
9		184.4	-0.087		-21793.6	21.777	-0.0054	valid
10		220.907	-0.105		-11902.2	11.955	-0.003	valid
11		157.611	-0.074		-13973	13.983	-0.0035	valid
12		186.184	-0.088		-11936.9	11.972	-0.003	valid
13		196.419	-0.093		-11066.4	11.111	-0.0028	valid
14		231.678	-0.11		-22346	22.35	-0.0056	valid
15		219.442	-0.104		-20194.3	20.203	-0.0051	valid
16		220.302	-0.105		-31769.1	31.718	-0.0079	valid
17		242.293	-0.116		-19493.6	19.517	-0.0049	valid
18		338.698	-0.164		-17911.2	17.991	-0.0045	valid
19		310.823	-0.149		-15827.3	15.904	-0.004	valid
20		243.493	-0.116		-17771.7	17.806	-0.0045	valid
21		-90.379	0.048		55076.34	-54.831	0.0136	invalid
22		194.459	-0.092		16150.05	-15.964	0.0039	valid

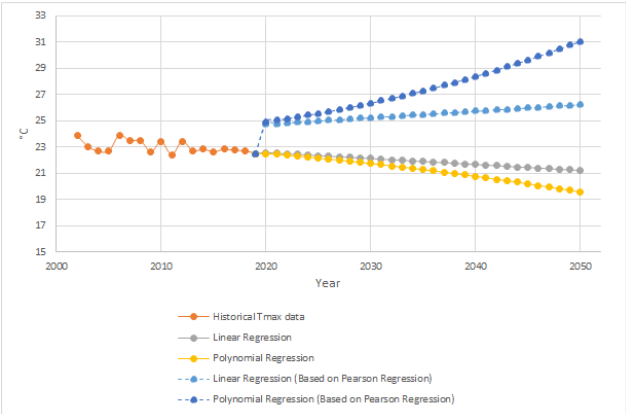

Figure 21: Predictive Tmin scenarios.

GDD

In analogy to the 3500 GDD noted in 2019, future results (Figure 22 and Table 13) have announced a general decrease in GDD values; LRM have a couple GDD values of 3308 and 3035 corresponding to 2034 and 2050, respectively. PLRM has a close result suggesting 3265 GDD in 2034 and 2968 by the year of 2050. PRM is being the most pessimistic case where GDD will be 3085 in 2034 and 2384 in 2050. As for PPRM, GDD will get 3087 in 2034 but it will be 2614 in 2050. Because it exclusively depends on Tmin and Tmax (Equation 2), it is certainly that GDD will have a similar trend to Tmin and Tmax. As a matter of fact, we want to see the future behavior of GDD based on forecasted Tmin and Tmax. The following map (Figure 23) give us the same future behavior but only with higher tendency. It is quite understandable because the simulations were made based on the resultant average diurnal temperatures from all the stations. Moreover, convenience of the results from Pearson correlation aren't the same for Tmin or Tmax. Lastly, variation of GDD will automatically confirm previous hypothesis about variation in diurnal temperatures. Thus, decreasing of GDD will modify the agricultural plant's phenology which will instable adequate crop yields for the growing population [54,55].

Table 13: Predictive GDD scenarios.

station	Linear			Poly (degree = 2)	Pear Corr			
	R^2	Alpha (intercept)	Beta (slope)	R^2	alpha	Beta 1	Bet 2	
1	0.4	13531.3	-5.024	0.41	3126827	-3102.08	0.77	valid
2		20773.23	-8.626		2559772	-2534.38	0.628	valid
3		38793.75	-17.588		392215.3	-369.166	0.087	valid
4		71485.76	-33.85		-3691948	3709.954	-0.931	valid
5		32539.12	-14.164		-1935656	1943.765	-0.487	valid
6		10966.17	-3.64		-137770	144.321	-0.037	valid
7		5889.645	-1.076		-93728.5	98.023	-0.025	valid
8		-3795.56	3.788		481207.5	-478.685	0.12	invalid
9		6616.811	-1.399		160202.4	-154.184	0.038	valid
10		44005.39	-20.068		-2265619	2277.509	-0.571	valid
11		60258.25	-28.223		-2642285	2660.224	-0.669	valid
12		63351.72	-29.712		-2617631	2637.287	-0.663	valid
13		53260.51	-24.612		-2383487	2399.426	-0.603	valid

14		2897 1.72	-12.4 66		-150 9492	1517. 973	-0.38 1	valid
15		2386 7.59	-9.92 3		-147 6167	1482. 287	-0.37 1	valid
16		4275 2.63	-19.4 5		-234 0001	2350. 875	-0.58 9	valid
17		6503 5.15	-30.5 31		-1179 970	1207. 98	-0.30 8	valid
18		1095 44.2	-52.6 75		-577 8356	5804. 514	-1.45 7	valid
19		7137 9.4	-33.5 85		-148 7837	1517. 498	-0.38 6	valid
20		3253 9.12	-14.1 64		-193 5656	1943. 765	-0.48 7	valid
21		1971 6.25	-7.93 8		-1.1 E+07	1084 5.73	-2.69 9	invali d
22		2403 5.59	-10.0 61		-130 2051	1309. 109	-0.32 8	valid

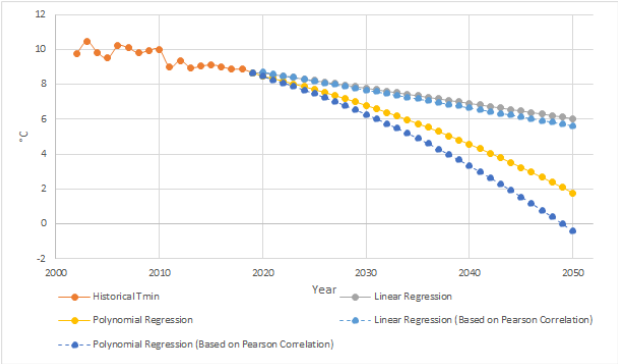

Figure 22: Predictive GDD scenarios.

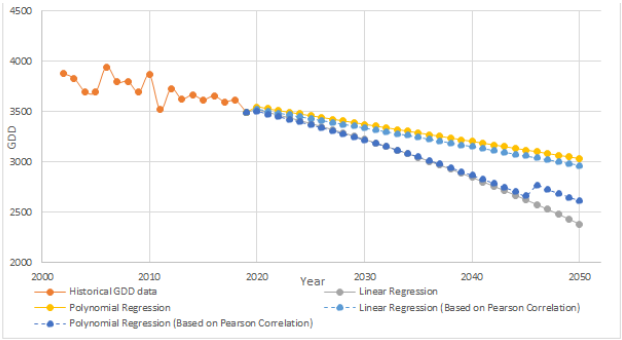

Figure 23: Simulated (based on Tmin and Tmax) and forecasted GDD.

Conclusion

The processing and the forecasting of LULC conversion as well as climate change scenarios have led to the assessment of the generated results:

- First LULC scenario has been limited only to major transition events. Due to that, some important patterns like urban areas and lakes has been neglected. As a result, assessment of future response to the climate change cannot be correctly assessed without taking in consideration the evolution of urban area.
- Assessment of both LULC scenarios is based on historical conversion trends of land use categories. Therefore, the second scenarios have revealed more pertinent results for all the classes.
- It is very difficult to predict weather change for a long period of time. For that, we have established four models to see all possible climate change scenarios.
- The four models were different in response going from one climate factor to the other. Although the coefficient of determination (R^2) is better with polynomial regression, but linear regression model seems to get the most coherent results (except of GDD).
- Pearson correlation has made future curves more oscillated which defines the standard behaviour of any weather parameter. In some cases, this correlation cannot be applied for stations with big variance in weather response.

References

1. Khoi DN & Suetsugi T (2014) The responses of hydrological processes and sediment yield to land-use and climate change in the Be River Catchment, Vietnam. Hydrol Process 28:640–652
2. Oliver TH & Morecroft MD (2014) Interactions between climate change and land use change on biodiversity: Attribution problems, risks, and opportunities. Wiley Interdisciplinary Reviews: Climate Change 5:317–335
3. Tan ML, Ibrahim AL, Yusop Z, Duan Z & Ling L (2015) Impacts of soil use and climate variability on hydrological components in the Johor River basin, Malaysia. Hydrol Sci J 60:873–889
4. Mendelsohn R & Dinar A (2009) Land Use and Climate Change Interactions. Annual Review of Resource Economics 1:309–332
5. Nobre CA, Sampaio G, Borma L S, Castilla-Rubio JC, Silva JS, et al. (2016) Land-use and climate change risks in the amazon and the need of a novel sustainable development paradigm. Proceedings of the National Academy of Sciences of the United States of America 113:10759–10768
6. World Resources Institue (2013) Aqueduct Country and River Basin Rankings 5:23-56
7. Weslati O, Bouaziz S, Serbaji MM (2020) Mapping and monitoring land use and land cover changes in Mellegue watershed using remote sensing and GIS. Arab J Geosci 13:58-75
8. Jazouli AEl, Barakat A, Khellouk R, Rais J & Baghdadi M El (2019) Remote sensing and GIS techniques for prediction of land use land cover change effects on soil erosion in the high basin of the Oum Er Rbia River (Morocco). Remote Sensing Applications: Society and Environment 13:361–374
9. Liping C, Yujun S & Saeed S (2018) Monitoring and predicting land use and land cover changes using remote sensing and GIS techniques—A case study of a hilly area, Jiangle, China. PLoS ONE 13:1–23
10. Wilson CO & Weng Q (2011) Simulating the impacts of future land use and climate changes on surface water quality in the Des Plaines River watershed, Chicago Metropolitan Statistical Area, Illinois. Science of the Total Environment 8:4387–4405

11. Hamad R, Balzter H & Kolo K (2018) Predicting land use/land cover changes using a CA-Markov model under two different scenarios. Sustainability (Switzerland) 10:1–23
12. Kumar S, Radhakrishnan N & Mathew S (2014) Land use change modelling using a Markov model and remote sensing. Geomatics, Natural Hazards and Risk 5:145–156
13. Ojima DS, Galvin Ka & Turner II BL (1994) The global impact of land-use change. to understand global change, natural scientists must consider the social context influencing human impact on environment. Bioscience 44:300–304
14. Abrahamsen EB, Brastein OM & Lie B (2018) Machine Learning in Python for Weather Forecast based on Freely Available Weather Data 8:26–28
15. Kadiyala A, Kumar A (2017) Applications of python to evaluate environmental data science problems. Environmental Progress & Sustainable Energy 36:1580-1586
16. Belloula M & Dridi H (2015) Modeling of the flows and solid transport in the catchment area of Meskiana-Mellegue upstream (Northeastern Algeria). Geographia Technica 10:1–7
17. Mlayah A, Ferreira da Silva E, Rocha F, Hamza C Ben, Charef A et al. (2009) The Oued Mellègue: Mining activity, stream sediments and dispersion of base metals in natural environments, North-western Tunisia. Journal of Geochemical Exploration 102:27–36
18. Thompson DWJ & Wallace JM (2000) Annular modes in the extratropical circulation. Part I: Month-to-month variability. Journal of Climate 13:1000–1016
19. WWC & AWC (2009) Vulnerability of arid and semi-arid regions to climate change. Impacts and adaptive strategies. Perspectives on water and climate change adaptation
20. Yang Z, Zhang Q, Hao X & Yue P (2019) Changes in Evapotranspiration Over Global Semiarid Regions 1984–2013. Journal of Geophysical Research: Atmospheres 124:2946–2963
21. Gibson L, Münch Z, Palmer A & Mantel S (2018) Future land cover change scenarios in South African grasslands – implications of altered biophysical drivers on land management. Heliyon 4:58-89
22. Mishra V, Rai P & Mohan K (2014) Prediction of land use changes based on land change modeler (LCM) using remote sensing: A case study of Muzaffarpur (Bihar), India. Journal of the Geographical Institute Jovan Cvijic, SASAZbornik Radova Geografskog Instituta Jovan Cvijic, SANU 64:111–127
23. Eastman JR (2006) Guide to GIS and Image Processing 9:0–327
24. Cartwright N, Clark L & Bird P (1991) The impact of agriculture on water quality. Outlook on Agriculture 20:145–152
25. Lawniczak AE, Zbierska J, Nowak B, Achtenberg K, Grześkowiak A, et al. (2016) Impact of agriculture and land use on nitrate contamination in groundwater and running waters in central-west Poland. Environmental Monitoring and Assessment 188:1–17
26. Van Der Werf HMG (1996) Assessing the impact of pesticides on the environment. Agriculture, Ecosystems and Environment 60: 81–96
27. Colazo JC & Buschiazzo D (2015) The Impact of Agriculture on Soil Texture Due to Wind Erosion. Land Degradation and Development 26:62–70
28. Skinner JA, Lewis KA, Bardon KS, Tucker P, Catt JA, et al. (1997) An overview of the environmental impact of agriculture in the UK. Journal of Environmental Management 50:111–128
29. Bennett EM (2017) Changing the agriculture and environment conversation. Nature Ecology and Evolution 1:1–2
30. Akram HM, Ali A, Sattar A, Rehman HSU & Bibi A (2013) Impact of water deficit stress on various physiological and agronomic traits of three Basmati rice (Oryza sativa L.) cultivars. Journal of Animal and Plant Sciences 23:1415–1423
31. Osakabe Y, Osakabe K, Shinozaki K & Tran LSP (2014) Response of plants to water stress. Frontiers in Plant Science 5:1–8
32. Pfister S & Bayer P (2014) Monthly water stress: Spatially and temporally explicit consumptive water footprint of global crop production. Journal of Cleaner Production 73:52–62
33. FAO (2003) FORESTS AND FORESTRY IN THE FUTURE: WHAT CAN WE EXPECT IN THE NEXT FIFTY YEARS? 9:56-69
34. INRAA (2007) National Report on the State of Phytogenic Resources for Food and Agriculture 44: 88-92
35. Cassagne JP (2017) Vegetative irrigation of fruit production 3:43-48
36. FAO (2015a) Oil field analysis. United Nations Food and Agriculture Organization 6:82-90
37. Commission E (2020) Market situation in the olive oil and table olives sectors Committee for the Common Organisation of the Agricultural Markets-Arable crops and olive oil 1:85-129
38. HuffPost Algeria (2015) Algeria 2nd producer, 5th exporter of wine in Africa and 11th consumer in the world | Al HuffPost Maghreb 1:87-108
39. Frida Dahmani (2010) Take the crosses from the bottle
40. McEwan A, Marchi E, Spinelli R & Brink M (2020) Past, present and future of industrial plantation forestry and implication on future timber harvesting technology. Journal of Forestry Research 31:339–351
41. CHRIHA S & SGHARI A (2013) Forest fires in Tunisia, irreversible sequelae of the revolution of 2011. Journal of Mediterranean Geography 121:87-93
42. FAO (2015b) EVALUATION DES RESSOURCES FORESTIERES MONDIALES 2015 - Algeria
43. Adam Mcquistan (2017) Using Machine Learning to Predict the Weather: Part 2 89:12-16
44. Lin P (2018) Impacts of climate change on reference evapotranspiration in the Qilian Mountains of China : Historical trends and projected changes 38:1–14
45. Roderick ML & Farquhar GD (2002) The Cause of Decreased Pan Evaporation over the past 50 Years. Science 298:1410–1411
46. Yao L (2017) Causative impact of air pollution on evapotranspiration in the North China Plain. Environmental Research 158:436–442
47. Ramarohetra J & Sultan B (2017) Impact of ET 0 method on the simulation of historical and future crop yields : a case study of millet growth in Senegal 38:729-741
48. HAUSFATHER Z (2018) Explainer: What climate models tell us about future rainfall. Carbon Brief 6:23-25
49. Fu P & Weng Q (2016) A time series analysis of urbanization induced land use and land cover change and its impact on land surface temperature with Landsat imagery. Remote Sensing of Environment 175:205–214

50. Jiang J & Tian G (2010) Analysis of the impact of Land use/Land cover change on Land Surface Temperature with Remote Sensing. Procedia Environmental Sciences 2:571–575

51. Zhang J, Dong W, Wu L, Wei J, Chen, P, et al. (2005) Impact of land use changes on surface warming in China. Advances in Atmospheric Sciences 22:343–348

52. Bernice Ackerman (1985) Temporal march of the Chicago heat island. Journal of Climate and Applied Meteorology 24:547-554

53. Anandhi A (2016) Growing degree days - Ecosystem indicator for changing diurnal temperatures and their impact on corn growth stages in Kansas. Ecological Indicators 61:149–158

54. Skaggs KE & Irmak S (2012) Long-term trends in air temperature distribution and extremes, growing degree-days, and spring and fall frosts for climate impact assessments on agricultural practices in Nebraska. Journal of Applied Meteorology and Climatology 51:2060–2073